Geophysical Research Letters

RESEARCH LETTER
10.1029/2022GL099871

Key Points:

- Shear wave splitting indicates strong anisotropy with an E-W fast direction just south of the Chile Triple Junction and the edge of the subducting Nazca slab
- The splitting and shear wave velocity structure suggest eastward shallow mantle flow in a 200–300 km wide channel around the edge of the Nazca slab
- In most of southernmost Patagonia, splitting shows NE-SW fast directions consistent with large-scale asthenospheric flow

Supporting Information:

Supporting Information may be found in the online version of this article.

Correspondence to:

W. Ben-Mansour,
walid.benmansour@seismo.wustl.edu

Citation:

Ben-Mansour, W., Wiens, D. A., Mark, H. F., Russo, R. M., Richter, A., Marderwald, E., & Barrientos, S. (2022). Mantle flow pattern associated with the Patagonian slab window determined from azimuthal anisotropy. *Geophysical Research Letters*, *49*, e2022GL099871. https://doi.org/10.1029/2022GL099871

Received 6 JUL 2022
Accepted 5 SEP 2022

Author Contributions:

Conceptualization: Walid Ben-Mansour, Douglas A. Wiens, Andreas Richter
Formal analysis: Walid Ben-Mansour
Funding acquisition: Douglas A. Wiens
Investigation: Walid Ben-Mansour, Douglas A. Wiens
Methodology: Walid Ben-Mansour
Supervision: Douglas A. Wiens
Writing – original draft: Walid Ben-Mansour
Writing – review & editing: Douglas A. Wiens, Hannah F. Mark, Raymond M. Russo, Andreas Richter

Mantle Flow Pattern Associated With the Patagonian Slab Window Determined From Azimuthal Anisotropy

Walid Ben-Mansour[1], Douglas A. Wiens[1], Hannah F. Mark[1,2], Raymond M. Russo[3], Andreas Richter[4], Eric Marderwald[4], and Sergio Barrientos[5]

[1]Department of Earth & Planetary Sciences, Washington University in Saint Louis, Saint Louis, MO, USA, [2]Woods Hole Oceanographic Institution, Woods Hole, MA, USA, [3]Department of Geological Sciences, University of Florida, Gainesville, FL, USA, [4]Laboratorio, MAGGIA, Universidad Nacional de La Plata, CONICET, La Plata, Argentina, [5]Centro Sismológico Nacional, Universidad de Chile, Santiago, Chile

Abstract Geological processes in Southern Patagonia are affected by the Patagonian slab window, formed by the subduction of the Chile Ridge and subsequent northward migration of the Chile Triple Junction. Using shear wave splitting analysis, we observe strong splitting of up to 2.5 s with an E-W fast direction just south of the triple junction and the edge of the subducting Nazca slab. This region of strong anisotropy is coincident with low uppermost mantle shear velocities and an absence of mantle lithosphere, indicating that the mantle flow occurs in a warm, low-viscosity, 200–300 km wide shallow mantle channel just to the south of the Nazca slab. The region of flow corresponds to a volcanic gap caused by depleted mantle compositions and absence of slab-derived water. In most of Patagonia to the south of this channel, splitting fast directions trend NE-SW consistent with large-scale asthenospheric flow.

Plain Language Summary Slab windows represent openings or gaps in the downgoing slab, allowing the mantle to flow through the plane of the slab from one side of the subduction zone to the other. The subduction of a spreading ridge beneath South America forms a gap in the subducting slab below Patagonia, presenting an opportunity to investigate the influence of slab windows on mantle flow and geological processes. Although this region has been poorly instrumented in the past, the deployment of new seismic instruments and available data allow us to study how the mantle seismic velocity varies with direction in the region. From the directional dependence of seismic velocity, we can infer the direction of mantle flow. We observe a change from N-S to E-W mantle flow in the northern part of the slab window, near the edge of the subducting Nazca plate. The flow occurs in a warm, low viscosity shallow mantle channel corresponding to a gap in activity along the volcanic arc.

1. Introduction

Slab windows, gaps between subducting slabs often formed by the subduction of spreading ridges, offer an important opportunity to study the relationship between tectonic processes and mantle dynamics. They produce local thermal anomalies and have strong physical and chemical effects on the surrounding mantle. The slab window perturbs mantle flow associated with subduction of oceanic lithosphere, producing toroidal flow around the edges of subducted slabs (Civello & Margheriti, 2004; Eakins et al., 2010; Peyton et al., 2001; Russo, Gallego, et al., 2010; Russo, Van Decar, et al., 2010). Such flow contributes to the thermal homogenization around the slab (Kincaid & Griffiths, 2004), and influences the temporal and spatial distribution of volcanism (Faccenna et al., 2010; Jadamec et al. (2010)) and mantle mixing (Guillaume et al., 2010). Slab windows provide an opportunity to study the strength and geographical pattern of toroidal flow at slab edges, as previously observed in the Mediterranean Sea (Civello & Margheriti, 2004) and the Western US (Zandt and Humphrey, 2008). Recently, Mark et al. (2022) proposed a thermal and mechanical erosion process to explain low mantle velocity anomalies and thinning of the lithospheric mantle between the Nazca slab edge and the northern part of the Patagonia slab window between 46° and 49°S. This observation raises questions related to the 3-D shape and strength of toroidal flow around the slab edge which could contribute to thermo-mechanical erosion of the lithosphere, and the potential influence of mantle flow patterns on surface volcanism.

The Patagonia slab window is the best current example of a migrating slab window, formed as the Chile Triple Junction (CTJ) between the Nazca, South American, and Antarctic Plates moved from south to north beginning

16 m.y. ago (Breitsprecher & Thorkelson, 2009). The CTJ has migrated ∼1000 km northward, as ridge segments subparallel to the trench collided with the subduction margin (Breitsprecher & Thorkelson, 2009). This evolution led to the formation of a gap in the subducting plate interface, allowing hot, buoyant, asthenospheric mantle to impinge on the South American plate from below, and producing mantle temperature and lithospheric thickness anomalies (Avila & Davila, 2018) as well as a gap in the active volcanic arc (Gutiérrez et al., 2005). Volcanism resumes south of the volcanic gap, but volcano spacing is larger, and plate boundary seismicity is reduced. South of 53° latitude, the plate boundary between the South.

American plate and the Scotia plate is defined by the Magallanes-Fagnano Fault System, a 600 km long continental transform fault with a slip rate of 0.7 cm/yr (Roy et al., 2020). The strike of the fault system gradually changes from NW-SE in the west to EW in Tierra del Fuego.

Early seismic studies have addressed the question of whether mantle flow between the Pacific and.

Atlantic oceans was occurring through the Patagonia slab window (Helffrich et al., 2002; Murdie & Russo, 1999; Russo, Gallego, et al., 2010; Russo, Van Decar, et al., 2010). From body wave tomography and shear wave splitting (SWS) analysis, Russo, Gallego, et al. (2010); Russo, Van Decar, et al. (2010) show the presence of a low seismic velocity anomaly and large SWS times near the CTJ. They also show variation in the fast direction of azimuthal anisotropy from ∼N to S north of the triple junction to ENE in the slab window. South of 51°S, Helffrich et al. (2002) show fast directions parallel to the absolute plate motion of the South American plate.

From the analysis of group velocities derived from ambient noise cross-correlation, Gallego et al. (2011) show the crust is affected by the slab window around 47°S, with relatively low shear wave velocity in comparison with the average velocity and significant anisotropy (1%–2%). P-receiver function analyses (Rodriguez & Russo, 2020) show crustal thickness increasing from south to north in the vicinity of the CTJ. Using a joint inversion of receiver functions and Rayleigh wave dispersion, Mark et al. (2022) found a pronounced thinning of the lithospheric mantle near the CTJ.

Here we present the results of a SWS analysis using SKS, SKKS, and PKS phases to characterize the mantle flow pattern beneath Southern Patagonia. We process broadband seismograms from the recent Glacial Uplift After Neoglaciation in the Andean Cordillera (GUANACO) temporary deployment (Mark et al., 2022) as well as previous deployments to measure shear-wave splitting parameters using the minimization of transverse component energy method (Silver and Chan, 1991). This new set of SWS measurements provides an extended view of the large-scale azimuthal anisotropy in southern South America and better constrains the mantle flow field associated with the Patagonia slab window. We then discuss the source of anisotropy in the context of the slab window, regional structure, subduction dynamics, and mantle flow patterns in Southern Patagonia.

2. Data Sets and Analysis

2.1. Broadband Seismic Data

Much of the data set comes from a recent deployment of the GUANACO temporary broadband network in Southern Patagonia. This network fills a data gap between the previous deployments in the CTJ region in the north (Russo, Van Decar, et al., 2010) and in southernmost Patagonia (Helffrich et al., 2002). The GUANACO network was deployed from November 2018 to February 2021 and consisted of 27 seismographs with station spacing of approximately 50–100 km (Mark et al., 2022). Additionally, we use all openly available broadband seismic data recorded in Southern Patagonia. These data come from Chilean broadband seismic networks (Chilean National Seismic Network, Red Sismológica Nacional); the 2004–2006 Chile Ridge Subduction Project (CRSP) (Russo, Van Decar, et al., 2010) and Seismic Experiment in the Aisen Region of Chile (SEARCH) data sets near the CTJ; and the 1997–1999 Seismic Experiment in Patagonia and Antarctica (SEPA) deployment in southernmost Patagonia (Helffrich et al., 2002). All the stations used in the analysis are shown in Figure 1.

2.2. Shear Wave Splitting Analysis

We perform SWS measurements on all high quality SKS, SKKS, and PKS phases recorded at stations in the study area. We selected earthquakes of Mw ≥ 5.7 at epicentral distances of 87°–140° from the study region for analysis. In the pre-processing, we apply different band-pass filters (6–50 s, 8–50 s, and 10–50 s) to find the optimum

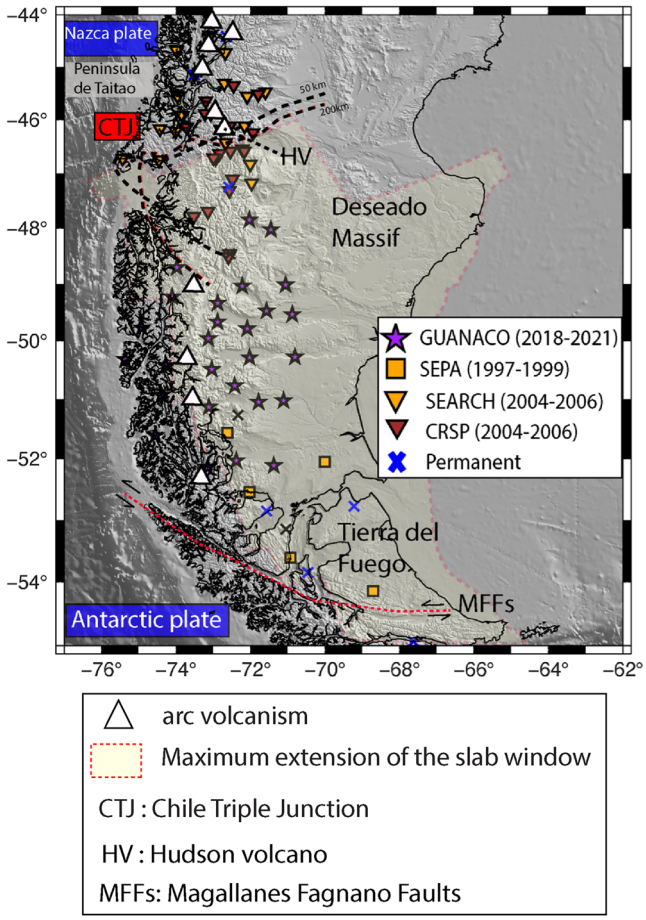

Figure 1. Topographic map of Southern Patagonia with main tectonic features showing seismic stations used for this study. The dashed lines represent the iso-depths (50 km in black and 200 km in red) defined by seismic velocity perturbation associated with the slab window (Russo, Van Decar, et al., 2010).

frequency range and we use a signal-to-noise cutoff ratio criteria to reject bad or ambiguous signals.

We first estimate the single-phase splitting parameter for each event at each station by using the energy minimization method (Silver and Chan, 1991) using the SplitRacer code (Reiss & Rümpker, 2017). This approach determines the best splitting parameters (fast direction and delay time) that minimize the energy on the transverse component. For each event and station, we assign a data quality (good-average-poor-null) based on different factors. A good signal to noise ratio and a narrow uncertainty associated with the splitting parameters estimations from the grid search are deemed to be good splitting measurements. Splitting measurements with good signal to noise ratio but relatively large uncertainty are deemed "average; " measurements showing no apparent splitting are referred to as "null." Null measurements most commonly arise when the fast or slow direction and the backazimuth of the event are very similar, so the shear wave is not split. We also deem measurements showing large uncertainties and small differences in the particle motion ellipticity pre and post rotation to be null. The choice of whether to assign a measurement to the "null" or "poor" categories depends on the signal-to-noise ratio and the ability to reduce the energy on the transverse component (see Supporting Information S1).

To compute the average splitting parameters for a given station, we use the joint-splitting analysis method implemented in SplitRacer (Reiss & Rümpker, 2017), which can reduce the influence of noise and provide a more robust measurement of the splitting beneath the station. In this approach, we apply the energy surface stacking method (Wolfe and Silver, 1998) to each phase and use only null and good split measurements from events recorded at a given station. We use a grid search to find the best splitting operator that minimizes the energy of the stacked transverse components. We then classify the quality of the resulting joint splitting results, relying on the number of phases analyzed and the uncertainties of the derived splitting parameters to quantify the average splitting parameter measurements as good, average, or poor. Joint analyses with very few phases and/or large splitting parameter uncertainties are defined as "poor." Null measurements are also identified when the energy on the transverse component cannot be reduced. Poor and null measurements are not shown on maps or used in the interpretation.

In addition, we also estimate the splitting intensity, defined as the amplitude ratio between the transverse component energy and the time derivative of the radial component energy (Chevrot, 2000; Monteiller & Chevrot, 2010). The results of the splitting intensity—where available—supplement the quality control of our splitting results.

3. Results

Results of individual and joint analysis of SWS parameters can be found in Supporting Information S1 (Table 1 in Supporting Information S1). From more than 480 individual splitting measurements, the final joint SWS parameters for individual stations comprise 33 good splits, 32 average splits and 16 null observations (Figure 2). Comparison of our measurements with previous analyses of open data sets for stations well north of the CTJ (Lynner & Beck, 2020) and in Tierra del Fuego (Helffrich et al., 2002) shows that we obtain similar results. Near the CTJ, our reprocessing of the Chile Ridge Subduction Project network shows some differences with previous studies (Russo, Van Decar et al., 2010). These differences can be attributed mainly to different choices in the selection and processing of core phases. The SWS results (Figure 2a) show four different domains, from north to south: (a) a region with variable but approximately N-S fast directions and small average splitting times north of the triple junction; (b) a region with E-W fast directions and larger splitting times near the CTJ between 46.5°S and 49°S; (c) much of southernmost Patagonia, showing NE-SW fast directions and generally modest (<1 s) splitting times; and (d) a limited region in Tierra del Fuego with small delay times with E-W fast directions.

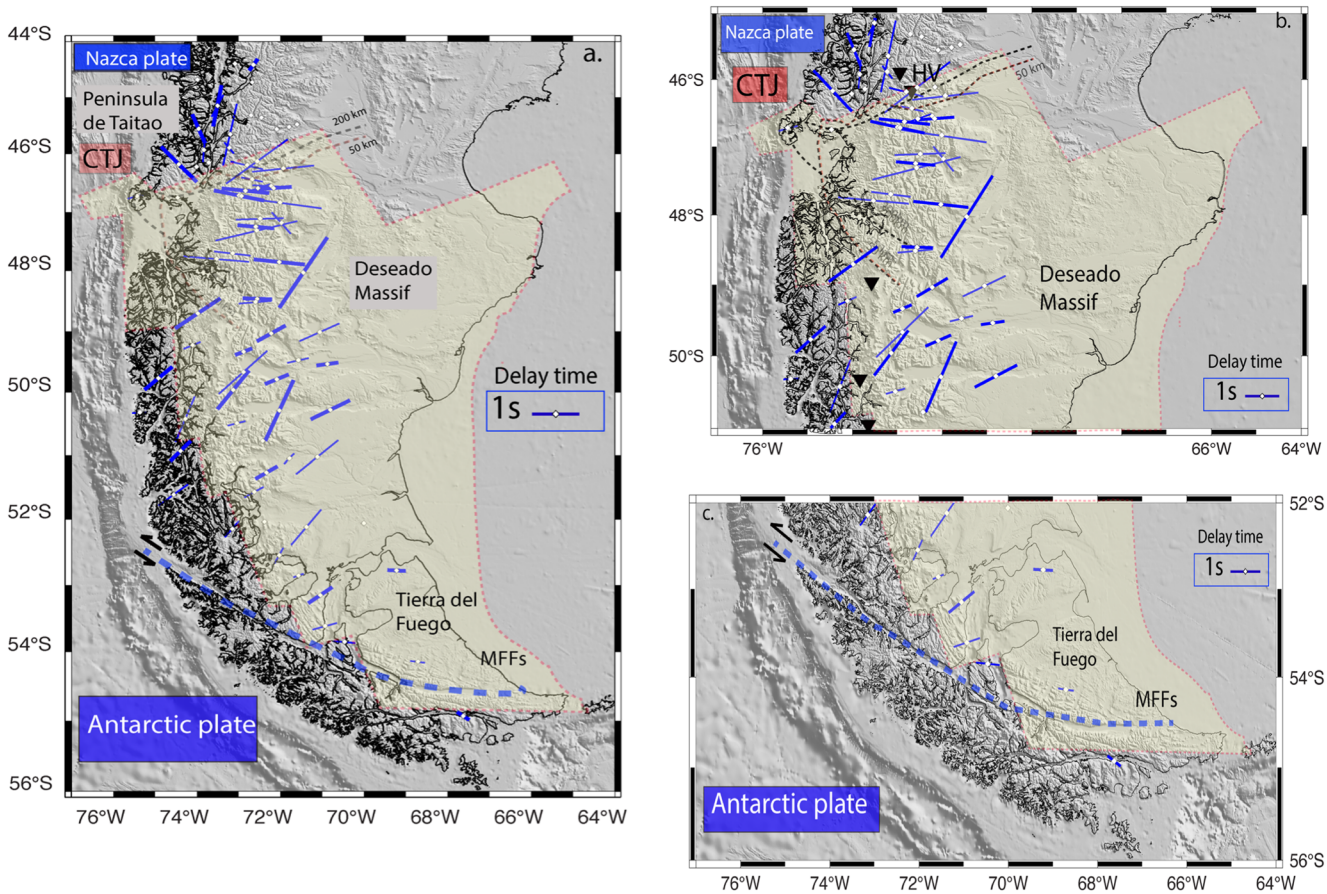

Figure 2. (a) Joint splitting results for the phases SKS-SKKS-PKS stacked at each station, assuming a single anisotropic layer. Thicker bars corresponding to good quality split measurements and thinner bars to average quality split measurements. (b) Enlarged view of the arc volcanism gap region and the edge of the Nazca slab (CTJ: Chilean Triple Junction; HV: Hudson Volcano). Active arc volcanoes are shown by triangles. (c) Enlarged view of the southernmost part of the continent (MFFs: Magallanes Fagnano Faults).

4. Discussion

4.1. Mechanism of Anisotropy

Anisotropy inferred from SKS splitting is generally interpreted as the consequence of the latticepreferred orientation (LPO) of olivine in the upper mantle, as the crust is typically too thin to accumulate significant splitting (e.g., Savage, 1999). However, both experimental geophysics and examination of mantle xenoliths show that olivine can form several different types of fabrics, making LPO interpretation more complex (Karato et al., 2008). Typically, in SWS studies, olivine A-type fabric, for which deformation aligns the crystallographic fast axis of olivine aggregates with the direction of maximum extension, is invoked, and observed fast splitting directions are assumed to be parallel to horizontal mantle flow.

Differences in water content, pressure-temperature condition and stress regime will affect the olivine fabric types present within the mantle, producing fabrics different from the A-type. For example, D-type fabrics, appropriate for dry, high stress conditions, can occasionally be observed within the lithosphere. C and E-type fabrics are sometimes found in the asthenosphere, where significant water content and low stress conditions are expected (Karato et al., 2008). However, these other fabrics result in SWS that is indistinguishable from A-type fabrics under horizontal flow conditions, and they are seldom invoked to explain teleseismic SWS measurements. One exception is B-type fabric, which is expected in regions with high water content and high stress (Karato et al., 2008), and has been used to explain trench-parallel SWS measurements in the supra-subduction mantle wedge regions of subduction zones (e.g., Long & Silver, 2008). Conditions in the slab window are unlikely to be conducive to development of B-type olivine fabrics, however, as the absence of a dehydrating slab, relatively high

temperatures due to asthenospheric inflow, and a relatively low stress regime except immediately adjacent to the lateral edge of the Nazca slab, are consistent with A-type or other fabrics with a fast direction parallel to the flow direction (Jung et al., 2006). Similar arguments apply to the asthenosphere throughout the region, which is likely to be too hot to allow B-type fabric to develop. The only exception is in the forearc, where lower temperatures and the presence of water may lead to B-type fabric (Karato et al., 2008). Thus, we assume A-type, or fabrics that have a similar splitting relationship, in this discussion, with the possible exception of the forearc.

4.2. Toroidal Flow in the Uppermost Mantle Around the Nazca Slab

Just to the south of the edge of the subducting Nazca slab, between 46°S and 49°S, we observe strong (delay times >2 s) SWS with an E-W fast-axes orientation (Figures 2a and 2b). This direction contrasts with N-S fast axes orientations north of the CTJ, and with NE-SW fast directions over most of the regions to the south which, as discussed below, likely reflects the average mantle flow direction in the region. We mapped larger splitting magnitudes (up to 2.5 s) in this area than elsewhere in the study region. The larger delay associated with the E-W fast direction compared to NE-SW fast directions elsewhere in Patagonia suggests vigorous toroidal mantle flow around the edge of the Nazca slab. Toroidal flow may also cause the plane of shear to be oriented vertically, in which case the fast and slow olivine axes are oriented subhorizontally, increasing the splitting magnitude relative to the typical assumption of horizontal shear planes (Faccenda & Capitanio, 2013).

The anisotropy observations constrain the direction of maximum shear strain but leave a 180° ambiguity in the direction of mantle flow. Russo and Silver (1994) suggested that mantle flow from the Pacific to the Atlantic upper mantle occurred beneath the Nazca slab and then through slab gaps in the Caribbean and Scotia regions based on observations of trench parallel patterns in azimuthal anisotropy. Russo, Van Decar, et al. (2010); Russo, Gallego, et al. (2010) observed trench-parallel splitting fast directions north of the slab window, modulating into more E-W splitting directions in the slab window itself. They interpreted these results as due to flow beneath the Nazca slab turning nearly 90° around the southern edge of the Nazca slab. This is consistent with recent modeling results suggesting mantle flow from the Pacific region to the Atlantic beneath Patagonia in the slab window region (Hu et al., 2017; Lin, 2014).

The region of inferred EW mantle flow around the Nazca slab coincides with a strong low velocity anomaly (Vsv < 4.1 km/s) in the uppermost mantle of the regional Vsv model (Mark et al., 2022).

The spatial distribution of E-W fast directions and low velocity uppermost mantle suggests the presence of a 200–300 km wide channel of vigorous flow at depths between 50 and 120 km (Figure 3). In the upper plate, high velocity mantle lithosphere is completely absent, and low velocity mantle extends upward nearly to the crust. Since the mantle lithosphere is present both north and south of this region, this indicates that the mantle lithosphere has been thermally and mechanically eroded in the youngest part of the slab window. Energetic flow of warmer mantle immediately beneath the colder mantle lithosphere thermally perturbed and weakened the lithosphere, with some small pieces likely detaching and being carried eastward by the flow.

In comparison with other regions where toroidal flow patterns are well mapped, such as in Western US near the Mendocino triple junction (Eakins et al., 2010) or in the Mediterranean Sea along the Calabria slab (Baccheschi et al., 2011), we don't observe the complete rotation of the fast direction. The lack of seismic instruments in the northernmost part of the backarc region in Argentina is a likely explanation for the incomplete rotation. The strong correlation between splitting delay times and low shear wave velocities is the common feature between Patagonia, Western US and the Mediterranean Sea, supporting the interpretation of strong toroidal flow.

A ~300 km gap in the arc volcanism occurs in the same northern slab window region (Figures 1 and 4) (Gutierrez et al., 2005). Plate reconstructions (Breitsprecher & Thorkelson, 2009), tomographic imaging (RussoVan Decar et al., 2010), and intermediate-depth seismicity show that the northern edge of the volcanic gap corresponds to the southern edge of Nazca slab. The location of the slab gap corresponds closely with the extent of the lowest upper mantle velocities (Mark et al., 2022) and the large E-W oriented fast anisotropy directions (Figures 2a and 2b). Modeling studies show that slab edges are generally characterized by toroidal flow, and that complex and vigorous mantle flow can control the temperature distribution around the slab as well as the location of surface volcanism (Faccenna et al., 2010; Jadamec et al., 2010; Kincaid & Griffiths, 2004). In the slab gap region, we are faced with an apparent discrepancy between vigorous mantle flow accompanied by very low upper mantle velocities, presumably reflecting elevated temperatures, and an absence of volcanism.

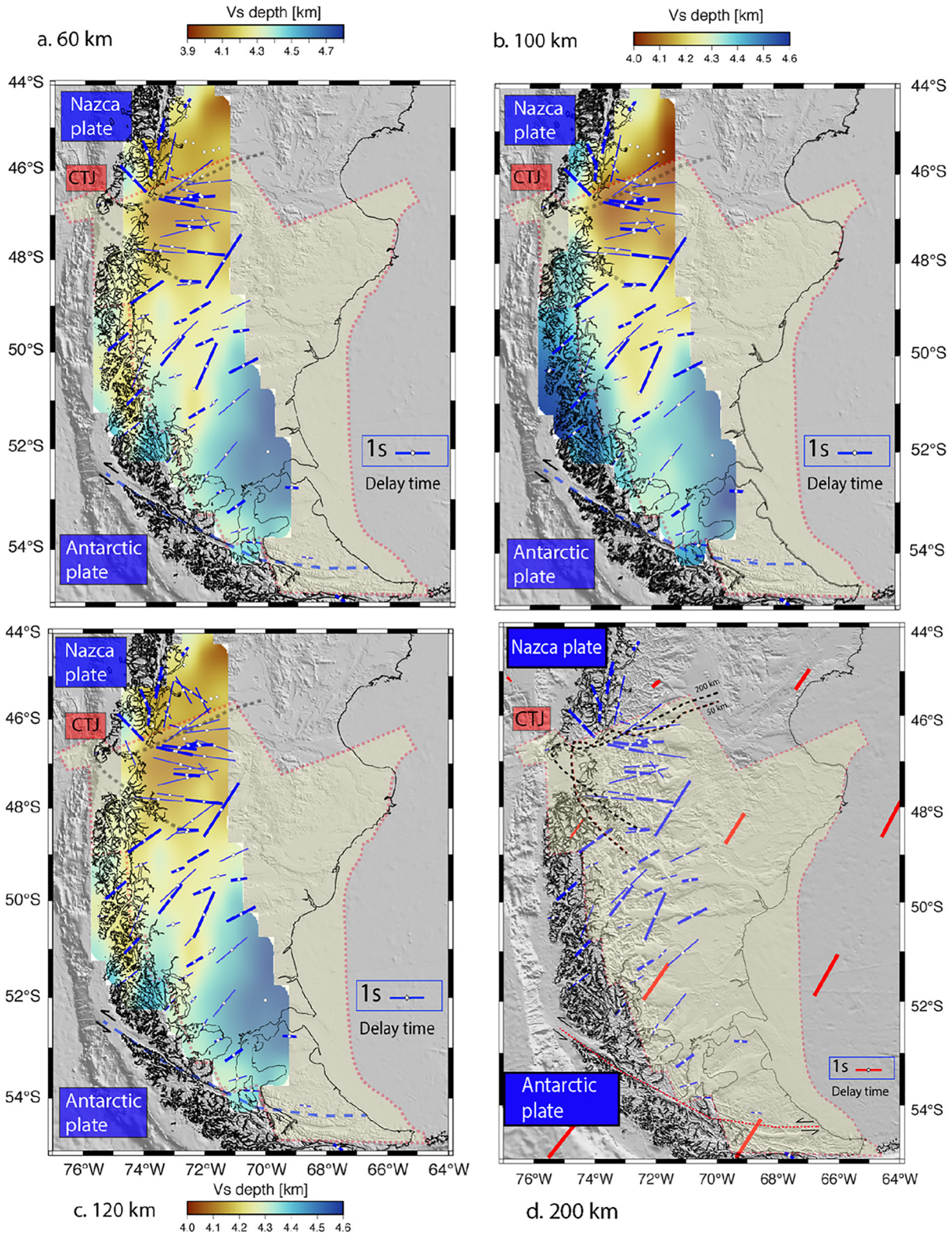

Figure 3. Comparison of the shear wave splitting results with the isotropic Vsv model (Mark et al., 2022) at (a) 60 km, (b) 100 km, (c) 120 km. and (d) fast directions from the global azimuthal shear velocity model SL2016svA (Schaeffer et al., 2016) at 200 km (red lines). Thicker bars are good splitting measurements and thinner bars are average.

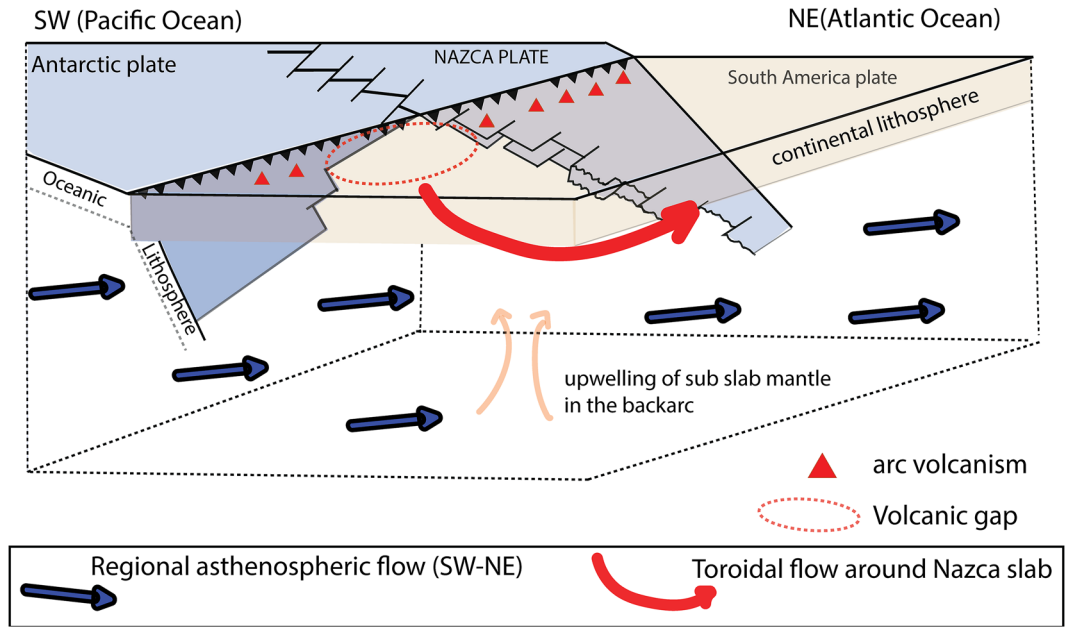

Figure 4. Illustration of the inferred mantle flow pattern near the Chile triple junction.

The most plausible explanation for the presence of the volcanic gap despite elevated mantle temperatures and vigorous mantle flow is the absence of slab-derived water necessary to generate melt, as well as depleted upper mantle compositions. Most arc magmas are produced by flux melting, as fluids released from the slab infiltrate the mantle wedge and lower the solidus (Grove et al., 2012; Sobolev and Chaussidon, 1996). In the absence of water from the slab, the upper mantle is likely similar to the mid-ocean ridge basalt (MORB) source region beneath the adjacent Chile Spreading Ridge, characterized by depleted compositions and low water contents. It is also likely that the vigorous west-to-east mantle flow in this region brings upper mantle material from beneath the Chile Spreading Ridge that has already undergone partial melting and extraction of water and incompatible elements, resulting in even stronger depletion in the slab gap. This results in a dry, depleted upper mantle incapable of melting even under the conditions of vigorous flow and elevated temperatures. There is petrological evidence for strong depletion in the slab gap area, as Hudson Volcano (Figure 1), the volcano bordering the gap on the northern side, is interpreted as erupting a depleted MORB-type component derived from the Chile Spreading Center (Gutierrez et al., 2005). High temperature upper mantle regions are often associated with decompression melting resulting from mantle upwelling. Numerical modeling (Kiraly et al., 2020) supports the idea of upwelling within a slab gap, but no arc volcanism is observed in the northern part of the slab window. Extensive backarc volcanism occurs in this area, and petrological studies show that decompression melting is the dominant mechanism (Gorring et al., 2001; Kay et al., 2013), suggesting that upwelling is concentrated in the backarc region.

4.3. Asthenospheric Flow in Southernmost Patagonia

Shear wave splitting directions are largely NE-SW throughout the region south of 49°S. This direction of observed splitting is aligned with the azimuthal anisotropy directions of the global model SL2016svA at depths of 150–200 km over a large region of Southern South America and the South Atlantic (Schaeffer et al., 2016) (Figures 3d and S3 in Supporting Information S1), and we interpret this anisotropy as resulting from large-scale flow in the asthenosphere (Figure 4). This direction is also similar to the present-day flow pattern predicted for this region by a geodynamical model using a tomography-based buoyancy structure (Hu et al., 2017).

Asthenospheric anisotropy—rather than lithospheric anisotropy—probably dominates the SWS measurements from Southernmost Patagonia due to the large inherent strength of asthenospheric anisotropy at those depths (Debayle & Ricard, 2013). The greater path length of the teleseismic shear waves in the asthenosphere relative to the mantle lithosphere, which is less than 100 km thick in this region (Mark et al., 2022), also implies an

asthenospheric source for the observed splitting. Comparison with a not-net rotation model (Argus et al., 2011) and a hot spot reference model (Gripp & Gordon, 2002) suggest a decoupling between absolute plate motion and the azimuthal anisotropy pattern in this region (see Figure S4 in Supporting Information S1). Thus, the anisotropy reflects active asthenospheric flow rather than passive shear deformation at the base of the lithospheric plates.

South of ~53.5° latitude, an E-W fast direction and smaller delay times (Figure 2c) suggest a different anisotropic domain relative to the NE-SW pattern observed from 49° to 53°S. Fast direction measurements for stations near the Magallanes-Fagnano fault (MFFs) zone are parallel to the fault zone, the South America-Scotia plate boundary, with about 1 cm/yr of nearly E-W strike slip motion (Mendoza et al., 2022). This observation suggests a relationship between the azimuthal anisotropy and this fault motion. Similar parallelism between azimuthal anisotropy has been observed at several other major strike-slip boundaries, such as the Alpine Fault in New Zealand, due to broad shear zones in the mantle beneath the fault (Zietlow et al., 2014).

5. Summary

The analysis of new data from seismic broadband instruments deployed in southern Patagonia between 2018 and 2021, along with open data from permanent stations and previous deployments, provides new constraints on the mantle flow pattern in this region. We develop a new SWS map using energy minimization and joint analysis techniques. This map shows large splitting delay times and E-W fast directions just south of the southern edge of the Nazca plate between 46°S and 49°S, coinciding with a region of very low uppermost mantle shear velocities. We interpret this as indicating a vigorous toroidal flow pattern in the uppermost mantle around the edge of the Nazca slab. Low seismic velocities co-located with the E-W fast directions imply high mantle temperatures, suggesting the flow has thermally and mechanically eroded the mantle lithosphere. The region of vigorous flow corresponds to a volcanic gap caused by the depletion of mantle compositions and an absence of water. A clear NE-SW fast direction from the SWS analysis in much of southernmost Patagonia reflects the regional asthenospheric flow. Near the Magallanes-Fagnano Fault accommodating South America-Scotia plate motion, splitting directions are E-W and parallel to the fault, consistent with deformation fabric produced by shear zones in the mantle beneath the fault.

Data Availability Statement

Data used in this study is from the GUANACO, SEPA, SEARCH and CRSP temporary seismic networks (network codes: 1P, 10/2018-03/2021; XB, 02/1997-10/1998; XJ, 12/2004-12/2006; YJ, 12/2004-12/2006), permanent stations from the Chile Network (network codes: C, C1). Data can be obtained from the IRIS Data Management Center (1P: https://www.fdsn.org/networks/detail/1P_2018/, XB: https://www.fdsn.org/networks/detail/XB_1997/,YJ: https://www.fdsn.org/networks/detail/YJ_2004/,C: https://www.fdsn.org/networks/detail/C/,C1: https://www.fdsn.org/networks/detail/C1/). Figures were produced using GMT software (Wessel et al., 2019). Seismic stations information, and shear wave splitting results presented in this contribution can be found in the Zenodo repository https://www.doi.org/10.5281/zenodo.5655438.

Acknowledgments
The authors thank Celeste Bollini, Gerardo Connon, Leticia Duca, Nora Sabbione, Patrick Shore, Gerd Sielfeld, Daniel Valladares, Martin Vazquez, and many others for their work in planning, deploying, servicing, and recovering the GUANACO seismic array. The authors thank reviewers for their thoughtful comments. Seismic instrumentation was provided by the Incorporated Research Institutions for Seismology (IRIS) through the PASSCAL Instrument Center at New Mexico Tech. Waveforms and metadata were accessed via the Incorporated Research Institutions for Seismology (IRIS) Data Management System. IRIS is funded by the Instrumentation and Facilities Program of the National Science Foundation. This research was funded by the National Science Foundation under grant EAR-1714154: Collaborative Research: Solid Earth Response of the Patagonian Andes to Post-Little Ice Age Glacial Retreat (https://www.nsf.gov/awardsearch/showAward?AWD_ID=1714154).

References

Argus, D. F., Gordon, R. G., & DeMets, C. (2011). Geologically current motion of 56 plates relative to the no-net-rotation reference frame. *Geochemistry, Geophysics, Geosystems*, *12*(11), Q11001. https://doi.org/10.1029/2011gc003751

Avila, P., & Davila, F. M. (2018). Heat flow and lithospheric thickness analysis in the Patagonian asthenospheric windows, southern South America. *Tectonophysics*, *747*, 99–107. https://doi.org/10.1016/j.tecto.2018.10.006

Baccheschi, P., Margheriti, L., Steckler, M. S., & Boschi, E. (2011). Anisotropy patterns in the subducting lithosphere and in the mantle wedge: A case study—The southern Italy subduction system. *Journal of Geophysical Research*, *116*, B08306. https://doi.org/10.1029/2010jb007961

Breitsprecher, K., & Thorkelson, D. J. (2009). Neogene kinematic history of NazcaAntarctic--Phoenix slab windows beneath Patagonia and the Antarctic Peninsula. *Tectonophysics*, *464*(1–4), 10–20. https://doi.org/10.1016/j.tecto.2008.02.013

Chevrot, S. (2000). Multichannel analysis of shear wave splitting. *Journal of Geophysical Research*, *105*(B9), 21579–21590. https://doi.org/10.1029/2000jb900199

Civello, S., & Margheriti, L. (2004). Toroidal mantle flow around the Calabrian slab (Italy) from SKS splitting. *Geophysical Research Letters*, *31*(10), L10601. https://doi.org/10.1029/2004gl019607

Debayle, E., & Ricard, Y. (2013). Seismic observations of large-scale deformation at the bottom of fast-moving plates. *Earth and Planetary Science Letters*, *376*, 165–177. https://doi.org/10.1016/j.epsl.2013.06.025

Eakins, C. M., Obrebski, M., Allen, R. M., Boyarko, D. C., Brudzinski, M. R., & Porritt, R. (2010). Seismic anisotropy beneath Cascadia and the Mendocino triple junction: Interaction of the subducting slab with mantle flow. *Earth and Planetary Science Letters*, *294*(3–4), 627–632. https://doi.org/10.1016/j.epsl.2010.07.015

Faccenda, M., & Capitanio, F. A. (2013). Seismic anisotropy around subduction zones: Insights from three-dimensional modeling of upper mantle deformation and SKS splitting calculations. *Geochemistry, Geophysics, Geosystems*, *14*(1), 243–262. https://doi.org/10.1002/ggge.20055

Faccenna, C., Becker, T. W., Lallemand, S., Lagabrielle, Y., Funiciello, F., & Piromallo, C. (2010). Subduction-triggered magmatic pulses: A new class of plumes? *Earth and Planetary Science Letters*, *299*(1–2), 54–68. https://doi.org/10.1016/j.epsl.2010.08.012

Gallego, A., Panning, M. P., Russo, R. M., Comte, D., Mocanu, V. I., Murdie, R. E., & Vandecar, J. C. (2011). Azimuthal anisotropy in the Chile Ridge subduction region retrieved from ambient noise. *Lithosphere*, *3*(6), 393–400. https://doi.org/10.1130/l139.1

Gorring, M. L., Matthew, L., & Kay, S. M. (2001). Mantle processes and sources of Neogene slab window magmas from southern Patagonia, Argentina. *Journal of Petrology*, *42*(6), 1067–1094. https://doi.org/10.1093/petrology/42.6.1067

Gripp, A. E., & Gordon, R. G. (2002). Young tracks of hotspots and current plate velocities. *Geophysical Journal International*, *150*(2), 321–361. https://doi.org/10.1046/j.1365-246x.2002.01627.x

Grove, T. L., Till, C. B., & Krawczynski, M. J. (2012). The role of H_2O in subduction zone magmatism. *Annual Review of Earth and Planetary Sciences*, *40*(1), 413–439. https://doi.org/10.1146/annurev-earth-042711-105310

Guillaume, B., Moroni, M., Funiciello, F., Martinod, J., & Faccenna, C. (2010). Mantle flow and dynamic topography associated with slab window opening: Insights from laboratory models. *Tectonophysics*, *496*(1–4), 83–98. https://doi.org/10.1016/j.tecto.2010.10.014

Gutierrez, F., Gioncada, A., Ferran, O. G., Lahsen, A., & Mazzuoli, R. (2005). The Hudson Volcano and surrounding monogenetic centres (Chilean Patagonia): An example of volcanism associated with ridge-trench collision environment. *Journal of Volcanology and Geothermal Research*, *145*(3–4), 207–233. https://doi.org/10.1016/j.jvolgeores.2005.01.014

Helffrich, G., Wiens, D. A., Vera, E., Barrientos, S., Shore, P., Robertson, S., & Adaros, R. (2002). A teleseismic shear-wave splitting study to investigate mantle flow around South America and implications for plate-driving forces. *Geophysical Journal International*, *149*(1), F1–F7. https://doi.org/10.1046/j.1365-246x.2002.01636.x

Hu, J., Faccenda, M., & Liu, L. (2017). Subduction-controlled mantle flow and seismic anisotropy in South America. *Earth and Planetary Science Letters*, *470*, 13–24. https://doi.org/10.1016/j.epsl.2017.04.027

Jadamec, M. A., Billen, M. I., & Magali, I. (2010). Reconciling surface plate motions with rapid threedimensional mantle flow around a slab edge. *Nature*, *465*(7296), 338–341. https://doi.org/10.1038/nature09053

Jung, H., Katayama, I., Jiang, Z., Hiraga, T., & Karato, S.-I. (2006). Effect of water and stress on the lattice-preferred orientation of olivine. *Tectonophysics*, *421*(1–2), 1–22. https://doi.org/10.1016/j.tecto.2006.02.011

Karato, S. I., Jung, H., Katayama, I., & Skemer, P. (2008). Geodynamic significance of seismic anisotropy of the upper mantle: New insights from laboratory studies. *Annual Review of Earth and Planetary Sciences*, *36*(1), 59–95. https://doi.org/10.1146/annurev.earth.36.031207.124120

Kay, S. M., Jones, H. A., & Kay, R. W. (2013). Origin of Tertiary to Recent EM-and subductionlike chemical and isotopic signatures in Auca Mahuida region (37--38 S) and other Patagonian plateau lavas. *Contributions to Mineralogy and Petrology*, *166*(1), 165–192. https://doi.org/10.1007/s00410-013-0870-9

Kincaid, C., & Griffiths, R. W. (2004). Variability in flow and temperatures within mantle subduction zones. *Geochemistry, Geophysics, Geosystems*, *5*(6), Q06002. https://doi.org/10.1029/2003gc000666

Kiraly, A., Portner, D. E., Haynie, K. L., Chilson-Parks, B. H., Ghosh, T., Jadamec, M., et al. (2020). The effect of slab gaps on subduction dynamics and mantle upwelling. *Tectonophysics*, *785*, 228458. https://doi.org/10.1016/j.tecto.2020.228458

Lin, S. C. (2014). Three-dimensional mantle circulations and lateral slab deformation in the southern Chilean subduction zone. *Journal of Geophysical Research: Solid Earth*, *119*, 3879–3896. https://doi.org/10.1002/2013jb010864

Long, M. D., & Silver, P. G. (2008). The subduction zone flow field from seismic anisotropy: A global view. *Science*, *319*(5861), 315–318. https://doi.org/10.1126/science.1150809

Lynner, C., & Beck, S. L. (2020). Subduction dynamics and structural controls on shear wave splitting along the South American convergent margin. *Journal of South American Earth Sciences*, *104*, 102824. https://doi.org/10.1016/j.jsames.2020.102824

Mark, H. F., Wiens, D. A., Ben Mansour, W., Ivins, E., Richter, A., Magnani, B. M., et al. (2022). Lithospheric erosion in the Patagonian slab window, and implications for glacial isostasy. *Geophysical Research Letters*, *49*(2), e2021GL096863. https://doi.org/10.1029/2021gl096863

Mendoza, L. P. O., Richter, A., Marderwald, E. R., Hormaechea, J. L., Connon, G., Scheinert, M., et al. (2022). Horizontal and vertical deformation rates linked to the Magallanes-Fagnano Fault, Tierra del Fuego: Reconciling geological and geodetic observations by modeling the current seismic cycle. *Tectonics*, *41*(1), e2021TC006801. https://doi.org/10.1029/2021tc006801

Monteiller, V., & Chevrot, S. (2010). How to make robust splitting measurements for single-station analysis and three-dimensional imaging of seismic anisotropy. *Geophysical Journal International*, *182*(1), 311–328. https://doi.org/10.1111/j.1365-246x.2010.04608.x

Murdie, R. E., & Russo, R. M. (1999). Seismic anisotropy in the region of the Chile margin triple junction. *Journal of South American Earth Sciences*, *12*(3), 261–270. https://doi.org/10.1016/s0895-9811(99)00018-8

Peyton, V., Levin, V., Park, J., Brandon, M., Lees, J., Gordeev, E., & Ozerov, A. (2001). Mantle flow at a slab edge: Seismic anisotropy in the Kamchatka region. *Geophysical Research Letters*, *28*(2), 379–382. https://doi.org/10.1029/2000gl012200

Reiss, M. C., & Rümpker, G. (2017). SplitRacer: MATLAB code and GUI for semiautomated analysis and interpretation of teleseismic shear-wave splitting. *Seismological Research Letters*, *88*(2A), 392–409. https://doi.org/10.1785/0220160191

Rodriguez, E. E., & Russo, R. M. (2020). Southern Chile crustal structure from teleseismic receiver functions: Responses to ridge subduction and terrane assembly of Patagonia. *Geosphere*, *16*(1), 378–391. https://doi.org/10.1130/ges01692.1

Roy, S., Vassallo, R., Martinod, J., Ghiglione, M., Sue, C., & Allemand, P. (2020). Co-seismic deformation and post-glacial slip rate along the Magallanes-Fagnano fault, Tierra Del Fuego, Argentina. *Terra Nova*, *321*, 1–10. https://doi.org/10.1111/ter.12430

Russo, R. M., Gallego, A., Comte, D., Mocanu, V. I., Murdie, R. E., & VanDecar, J. C. (2010). Source-side shear wave splitting and upper mantle flow in the Chile Ridge subduction region. *Geology*, *38*(8), 707–710. https://doi.org/10.1130/g30920.1

Russo, R. M., & Silver, P. (1994). Trench parallel flow beneath the Nazca plate from seismic anisotropy. *Science*, *263*(5150), 1105–1111. https://doi.org/10.1126/science.263.5150.1105

Russo, R. M., Van Decar, J. C., Comte, D., Mocanu, V. I., Gallego, A., & Murdie, R. E. (2010). Subduction of the Chile Ridge: Upper mantle structure and flow. *Geological Society of America Today*, *20*(9), 4–10. https://doi.org/10.1130/gsatg61a.1

Savage, M. K. (1999). Seismic anisotropy and mantle deformation: What have we learned from shear wave splitting? *Reviews of Geophysics*, *37*(1), 65–106. https://doi.org/10.1029/98rg02075

Schaeffer, A. J., Lebedev, S., & Becker, T. W. (2016). Azimuthal seismic anisotropy in the Earth's upper mantle and the thickness of tectonic plates. *Geophysical Supplements to the Monthly Notices of the Royal Astronomical Society*, *207*(2), 901–933. https://doi.org/10.1093/gji/ggw309

Silver, P. G., & Chan, W. W. (1991). Shear wave splitting and subcontinental mantle deformation. *Journal of Geophysical Research*, *96*(B10), 16429–16454. https://doi.org/10.1029/91jb00899

Sobolev, A. V., & Chaussidon, M. (1996). H2O concentrations in primary melts from supra-subduction zones and mid-ocean ridges: Implications for H_2O storage and recycling in the mantle. *Earth and Planetary Science Letters*, *137*(1–4), 45–55. https://doi.org/10.1016/0012-821x(95)00203-o

Wessel, P., Luis, J. F., Uieda, L., Scharroo, R., Wobbe, F., Smith, W. H. F., & Tian, D. (2019). The generic mapping tools version 6. *Geochemistry, Geophysics, Geosystems*, *20*(11), 5556–5564. https://doi.org/10.1029/2019gc008515

Wolfe, C. J., & Silver, P. G. (1998). Seismic anisotropy of oceanic upper mantle: Shear wave splitting methodologies and observations. *Journal of Geophysical Research*, *103*(B1), 749771–771. https://doi.org/10.1029/97jb02023

Zandt, G., & Humphreys, E. (2008). Toroidal mantle flow through the western US slab window. *Geology*, *36*(4), 295–298. https://doi.org/10.1130/g24611a.1

Zietlow, D. W., Sheehan, A. F., Molnar, P. H., Savage, M. K., Hirth, G., Collins, J. A., & Hager, B. H. (2014). Upper mantle seismic anisotropy at a strike-slip boundary: South Island, New Zealand. *Journal of Geophysical Research: Solid Earth*, *119*, 1020–1040. https://doi.org/10.1002/2013jb010676